ELSEVIER

Journal of Inorganic Biochemistry 84 (2001) 171–178

JOURNAL OF Inorganic Biochemistry

www.elsevier.nl/locate/jinorgbio

Structural correlation of catecholase-like activities of oxy-bridged dinuclear copper(II) complexes

Chia-Horng Kao[a], Ho-Hsiang Wei[a,*], Yi-Hung Liu[b], Gene-Hsiang Lee[b], Yu Wang[b], Chin-Jhan Lee[c]

[a]*Department of Chemistry, Tamkang University, Tamsui 25137, Taiwan*
[b]*Instrumentation Center, College of Science, National Taiwan University, Taipei, Taiwan*
[c]*Deh-Yu College of Nursing and Management, Keelung, Taiwan*

Received 8 August 2000; received in revised form 29 December 2000; accepted 2 January 2001

Abstract

Eight oxy-bridged dinuclear copper(II) complexes with catecholase-like sites, $[Cu(L^1)X]_2$ (HL^1=1-diethylaminopropan-2-ol, $X=N_3^-$ **1**, NCO^- **2**, and NO_2^- **3**), $[Cu(L^2)X]_2$ (HL^2=*N*-ethylsalicylaldimine, $X=NO_3^-$ **4**, Cl^- **5**, N_3^- **6**, NCS^- **7**), and $[Cu(L^3)]_2(ClO_4)_2$ **8** (HL^3=*N*-(salicylidene)-*N′*-(2-pyridylaldene)propanediamine) have been prepared and characterized. The single crystal X-ray analysis show that the structures of complexes **6** and **8** are dimeric with two adjacent copper(II) atoms bridged by pairs of μ-oxy atoms from the L^2 and L^3 ligands. Magnetic susceptibility measurements in the temperature range 4–300 K indicate significant antiferromagnetic coupling for **4**, **5** and **7** and ferromagnetic coupling for **6** between the copper(II) atoms. The catecholase activity of complexes for the oxidation of 3,5-di-*tert*-butylcatechol by O_2 was studied and it was found that the complexes with the bond distance of Cu(II)···Cu(II) located at 2.9–3.0 Å show higher catecholase activity.

Keywords: Copper complexes; Catecholase activity; Oxy atoms

1. Introduction

Dinuclear copper active centers play an important role in biological metalloenzymes [1–10]. The best investigated binuclear copper(II) proteins are hemocyanin [5], and tyrosinase [6–10] or catechol oxidase [11,12]. Tyrosinase catalyses the aerial oxidation of monophenols to *o*-diphenols (cresolase activity) and the oxidation of *o*-phenols (catechols) to *o*-quinones (catecholase or diphenolase activity). The crystal structure of tyrosinase has not been determined, but spectroscopic studies seem to reveal that the active site is similar to that of hemocyanin [6–10]. Extended X-ray absorption fine structure (EXAFS) measurements for the *met*-tyrosinase give a Cu···Cu distance of 3.4 Å. Spectroscopic studies on the native *met* form of catecholase from *Lycopus europaeus* and *Ipomoea batatas* have revealed that the active site consists of two copper atoms with the Cu···Cu distance of 2.9 Å. Where the metals are coordinated by four N/O donor ligands [11,12]. Recently, Krebs and co-workers [13–15] have reported the crystal–structural and EXAFS studies on the deoxy, met, and inhibitor-bound forms of catecholoxidase (COases) from *Ipomoea batatas* (sweet potato), and revealed the binuclear copper active site of the O_2 form has a Cu···Cu distance of 3.8 Å.

The catecholase-like active model binuclear copper(II) complexes with different structural parameters have been investigated [6–10]. Nishida et al. [16] have found that several oxy-bridged binuclear Cu(II) complexes show catalytic activity if the Cu···Cu distance is less than 5 Å. A steric match between substrate and complex is believed to be important determined by the factors that two metal centres have to be located in proximity to facilitate binding of two hydroxyl oxygen atoms of catechol prior to the electron transfer [17–21]. Krebs and co-workers [21,22] reported structural correlations of catecholase activity in phenoxy- and alkoxy-bridged dinuclear Cu(II) complexes. Recently, Casella and co-workers [23,24] undertook a detailed mechanistic and electrochemical investigation on the catecholase activity of a group of model binuclear copper complexes.

We reported on the magnetostructural correlations and

*Corresponding author. Tel.: +886-2-2621-5656; fax: +886-2-2620-9924.

E-mail address: tkwei@mail.tku.edu.tw (H.-H. Wei).

0162-0134/01/$ – see front matter
PII: S0162-0134(01)00170-2

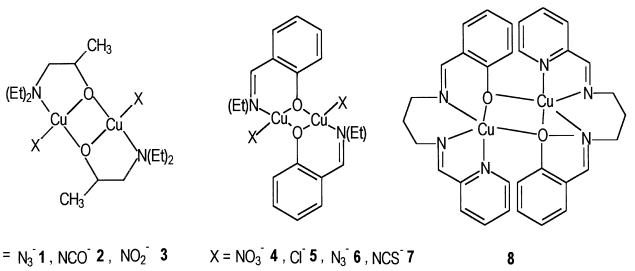

Scheme 1. Scheme for oxy-bridged binuclear copper(II) complexes.

catecholase-like alkoxy-bridged dinuclear copper(II) complexes, $[Cu(L^1)X]_2$ (HL^1=1-diethylaminopropan-2-ol, X= N_3^-, NCO^-, and NO_2^-) [25]. The results revealed the trend of catecholase-like activity correlated to the sort of anion X^- and the Cu···Cu distance in these complexes. In this contribution, we have been particularly interested in systematic investigations on the binuclear copper(II) complexes as structural and functional models for catecholase. Here we report an investigation of the structural correlation between catecholase-like activity and the Cu–Cu distance of a series of oxy-bridged binuclear copper(II) complexes (see Scheme 1) with HL^1 (=1-diethylaminopropan-2-ol), HL^2 (=*N*-ethyl-2-hydroxybenzylidenimine), and HL^3 (=*N*-(salicylidene)-*N′*-(2-pyridylaldene)propanediamine). In general, a way to get a short metal–metal distance in a model dicopper(II) complex, which is close to the Cu–Cu distance of 2.9 Å in native catecholase and enables strong magnetic coupling, is by using dimeric ligands with a bridging alcoholate or phenolate oxygen atoms.

2. Experimental

2.1. Syntheses

2.1.1. $[Cu(L^1)X]_2$, $X=N_3^-$ **1**, NCO^- **2**, NO_2^- **3**

The preparations and characterizations of complexes **1**–**3** have been described elsewhere [25].

2.1.2. $[Cu(L^2)X]_2$, $X=NO_3^-$ **4**, Cl^- **5**, N_3^- **6**, and NCS^- **7**

The complexes **4** and **5** are prepared in the same manner using modification of a literature method [26,27]. To a solution of salicylaldehyde (610 mg, 5 mmol) and ethylamine (225 mg, 5 mmol) in warm methanol (20 cm^3) was added a solution of anhydrous copper(II) nitrate (10 mmol) or copper(II) chloride (10 mmol) in methanol (20 cm^3). The solution was heated to boiling with stirring and stood at room temperature for several days. A black precipitate was obtained and single crystal of **4** or **5** was grown in DMF solution. (Found: C, 39.30; H, 3.68; N, 10.09. Calc. for $[C_{18}H_{20}Cu_2N_4O_8]$ (**4**): C, 39.42; H, 3.70; N, 10.22%. Found: C, 43.54; H, 4.10; N, 5.45. Calc. for $[C_{18}H_{20}Cl_2Cu_2N_2O_2]$ (**5**): C, 43.72; H, 4.05; N, 5.67%).

The complexes **6** and **7** were prepared in the same manner as follows: To a methanolic solution (20 cm^3) of salicylaldehyde (2.0 mmol), ethylamine (2.0 mmol) and copper(II) acetate monohydrate (400 mg, 2.04 mmol), a methanol solution of (10 cm^3) sodium azide (132.8 mg, 2.04 mmol) or potassium thiocyanate (198.3 mg, 2.04 mmol) was added. The reaction mixture was allowed to stand at 25°C for several days. Dark black single crystals formed, and were filtered off and dried in vacuum. (Found: C, 42.47; H, 3.98; N, 21.94. Calc. for $C_{18}H_{20}Cu_2N_8O_2$ (**6**): C, 42.52; H, 3.94; N, 22.05%. Found: C, 44.43; H, 3.58; N, 10.29. Calc. for $C_{20}H_{20}Cu_2S_2N_4O_2$ (**7**): C, 44.44; H, 3.70; N, 10.37%).

2.1.3. $[Cu(L^3)]_2(ClO_4)_2$ **8**

A mixture of salicylaldehyde (610 mg, 5 mmol) and propanediamine (370 mg, 5 mmol) in CH_2Cl_2 25 cm^3 was stirred for 24 h. During this time the solution turned a yellow. The solution was evaporated to dryness. Then the residue was dissolved in 15 cm^3 of CH_3OH. To this yellow solution, a solution of 2-pyridinecarboxaldehyde (535 mg, 5 mmol) in 15 cm^3 of CH_3OH was added. The mixture was stirred at 50°C for 1 h and a solution of $Cu(ClO_4)_2 \cdot 6H_2O$ (3.70 g, 10 mmol) (***caution***: perchlorates may explode violently) in 15 cm^3 CH_3OH was slowly added. The combined solution was stirred at room temperature for 2 h, and was reduced in volume to 15 cm^3. On allowing the solution to stand for several days, dark brown crystals of complex **8** suitable for X-ray analysis were obtained. (Found: C, 44.91; H, 3.82; N, 9.72. Calc. for $C_{32}H_{32}Cl_2Cu_2N_6O_{10}$ (**8**): C, 44.76; H, 3.73; N, 9.79%).

2.2. Physical measurements

The temperature dependence of the magnetic susceptibility of polycrystalline samples of **6**–**8** was measured between 5 and 300 K at a field of 1 T using a Quantum Design model MPMS computer-controlled SQUID magnetometer. Diamagnetic corrections were made using Pascal's constants [28]. X-band ESR spectra at 300 K for the complexes in the form of solid state and in methanol solution were examined on a Brucker ESC-106 spectrometer. Electronic spectra were recorded on a Cintra 20 UV-Visible spectrometer.

2.3. Crystallography

The molecular structures of complexes **1**–**5** determined by X-ray single crystal analyses are known. Here the X-ray data for complexes **7** and **8** were collected on a Siemens P4 and an Enraf–Nonius CAD4 X-ray diffractometer, respectively, with graphite-monochromatized Mo Kα radiation at 25°C. The unit cell parameters were deter-

Table 1
Crystallographic data for the complexes

	7	8
Empirical formula	$C_{20}H_{20}Cu_2N_4O_2S_2$	$C_{32}H_{32}Cu_2N_6O_{10}Cl$
M	639.60	858.62
Crystal system	Monoclinic	Monoclinic
Space group	$C2/c$	$P2_1/n$
a (Å)	18.788(3)	12.381(3)
b (Å)	9.4607(7)	7.0417(14)
c (Å)	15.429(3)	19.494(4)
β (°)	125.741(10)	90.50(3)
V (Å^3)	2226.0(6)	1699.5(6)
Z	4	4
D_c (g cm^{-3})	1.610	1.678
F(000)	1096	876
λ (Å)	0.7107	0.7107
No. measured reflections	2025	2985
No. observed reflections	1963	2985
R_f [a]	0.0336a	0.0414
R_w [b]	0.0827	0.0953

[a] $R_f = \sum(|F_o| - |F_c|)/\sum|F_o|$.
[b] $R_w = \{w(F_o^2 - F_c^2)^2/\sum[w(F_o)^4]\}^{1/2}$.

mined from $2.53° < \theta < 25°$ for **7**, and $11.94 < \theta < 24.97°$ for **8**. The details of data collection, crystallographic data, and reduction are summarized in Table 1. The structures of **7** and **8** were solved by standard direct methods and refined by full-matrix least-squares based on F^2 using the SHELX-93 computer program package [29]. All non-hydrogen atoms were refined anisotropically. Selected bond distances and angles of **7** and **8** are listed in Table 2.

2.4. Catecholase-like activity measurements

Electronic spectra at 25°C were recorded for complexes **1**–**8** in methanol and their catalytic activity for the oxidation of 3,5-di-*tert*-butylcatechol (H_2dtbc) with O_2 in methanol monitored on a UV-Visible spectrometer. The reaction with H_2dtbc was studied at 25°C by adding equivalent catechol solutions to the same amounts of the complexes and by recording the spectra at different time intervals. The yield of quinone formed in the oxidation in methanol was determined from the measured absorbances at about 400 nm of the resulting solutions [16,25].

3. Results and discussion

3.1. Description of the crystal structures

The crystal structures of **1**–**3** [25], **4** [30], and **5** [31] have been reported previously. Here crystal structures of complexes **7** and **8** were determined. In general, all consist of dinuclear complexes in which the copper centres are bridged by the alkoxy (for complexes **1**–**3**) and phenoxy (for complexes **4**–**5**, and **7**–**8**) groups of the ligands. The structures of complexes **7** and **8** are shown in Figs. 1 and 2, and selected bond distances and angles are given in Table 2.

3.2. $[CuL^2(NCS)]_2$ 7

The overall structural characteristic for complex **7** is substantially similar to those reported for complexes **4** [30] and **5** [31]. The coordination geometry around the copper atom is distorted square planar, and is formed by two phenoxy oxygen atoms, an imino nitrogen atom, and a nitrate nitrogen atom for **4**, a chloro atom for **5**, and thiocyanate nitrogen atom for **7**. Although the structure of **7** consists essentially of phenoxy bridged centrosymmetric

Table 2
Selected bond distances (Å) and angles (°) for complexes **7** and **8**

Compound **7**			
Cu(1)···Cu(1a)	3.0575(8)	Cu(1)–O(1)	1.932(2)
Cu(1a)–O(1a)	1.994(2)	Cu(1)–N(1)	1.987(3)
Cu(1)–N(2)	1.934(3)	C(1)–O(1)	1.334(4)
Cu(1)···Cu(1a)	3.0575(8)	Cu(1)···S(1)	2.7191(10)
Cu(1)–O(1)–Cu(1a)	102.32(9)	O(1)–Cu(1)–N(2)	170.71(11)
O(1)–Cu(1)–N(1)	89.32(10)	N(2)–Cu(1)–N(1)	97.32(12)
O(1)–Cu(1)–O(1a)	75.66(10)	N(2)–Cu(1)–O(1a)	95.57(11)
N(1)–Cu(1)–O(1a)	151.32(11)	O(1)–Cu(1)–S(1)	89.08(7)
N(2)–Cu(1)–S(1)	96.02(9)	N(1)–Cu(1)–S(1)	100.70(9)
C(10)–N(2)–Cu(1a)	166.6(3)	N(2)–C(10)–S(1)	179.4(3)
Compound **8**			
Cu(1)···Cu(1a)	3.3784(12)	Cu(1)–O(1)	1.894(3)
Cu(1)–O(1a)	2.695(5)	Cu(1)–N(1)	2.013(3)
Cu(1)–N(2)	1.991(4)	Cu(1)–N(3)	1.952(3)
Cu(1)–O(1)–Cu(1)	93.22(14)	O(1)–Cu(1)–N(2)	169.61(13)
N(1)–Cu(1)–N(3)	169.7(2)	O(1)–Cu(1)–N(1)	89.31(13)
N(2)–Cu(1)–N(3)	96.3 (2)	O(1)–Cu(1)–N(3)	94.07(13)
O(1)–Cu(1)–O(1a)	86.78(12)		

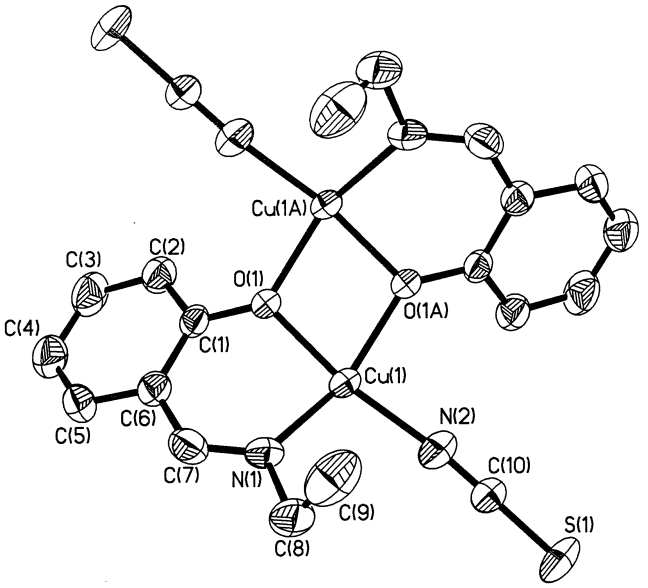

Fig. 1. Molecular structure and atomic numbering scheme for **7**.

binuclear units, nevertheless, the binuclear units are further associated by bridging thiocyanate groups to yield a one-dimensional chain (see Fig. 3). The resulting Cu···Cu bond distance, 3.0575(8) Å and the Cu–O–Cu bond angle, 102.32(9)° of **7** are slightly larger than those of 3.008(1) Å and 101.1(1)° for **4** [30], 3.051(1) Å and 103.3° for **5** [31], respectively.

3.3. $[Cu(L^3)]_2(ClO_4)_2$ ***8***

The structure of complex **8** illustrated in Fig. 2 consists of oxygen-bridged dimers with a distorted square-pyramidal geometry at the copper atoms and an out-of plane Cu–O distance of 2.695(3) Å. The presence of an axial oxygen atom leads to an intradimer Cu···Cu distance of 3.378 Å, longer than in **1** (2.807), **2** (2.869), **3** (2.928), **4** (3.008), **5** (3.051), or **7** (3.058 Å).

3.4. Magnetic properties

The solid state temperature dependence of magnetic data

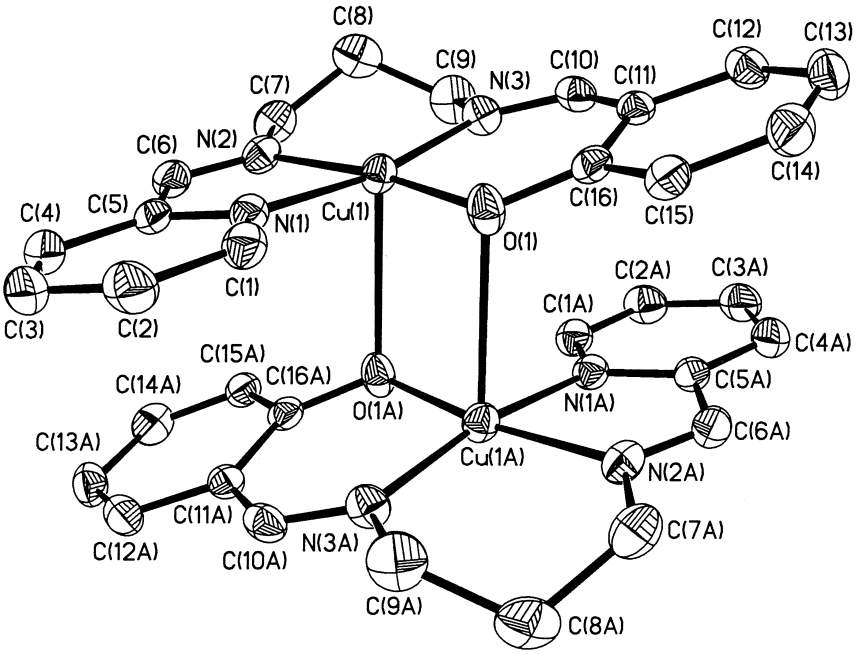

Fig. 2. Molecular structure and atomic numbering scheme for **8**. The ClO_4^- is omitted for clarity.

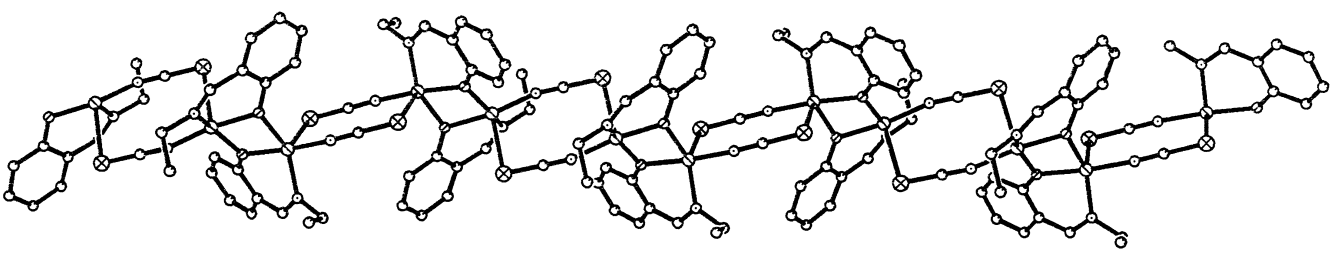

Fig. 3. Quasi-polymer chain structure of **7** with NCS^- self-assembly.

for complexes **1**–**5** were reported previously [25,30]. Here solid state magnetic susceptibility measurements on polycrystalline samples of **6**–**8** were made in the temperature range between 5 and 300 K. For complexes **6** and **7** the obtained values and curves of $\chi_m T$ versus temperature are typical for weak ferromagnetic and strong antiferromagnetic coupling between two $S=1/2$ copper(II) ions in dinuclear complexes. Whereas for complex **8** the obtained values and curve of $\chi_m T$ versus temperature is typical for very weak magnetic coupling between two Cu(II) ions which obey the Curie–Weiss law with $\theta=-0.4$ K. The representative $\chi_m T$ and χ_m versus T data for **6** are shown in Fig. 4. The room temperature values for $\chi_m T$ are 0.71 cm^{-3} K mol^{-1} for **6** and 0.21 cm^{-3} K mol^{-1} for **7**, respectively. The $\chi_m T$ values for **6** increase at 12 K to ca. 1.35 cm^{-3} K mol^{-1}, and for **7** decrease at 5 K to ca. 0.02 cm^{-3} K mol^{-1}, respectively. The values for **7** could be fitted on the basis of an isotropic Heisenberg model, $H=-2JS_1S_2$ [32], and for **6** could be fitted on the basis of anisotropic interactions in copper(II) binuclear moiety which take the form $H=-2JS_1S_2+S_1DS_2$ [33]. The best parameters obtained were as follows: for **7**, $g=2.05$, $2J=-320(10)$ cm^{-1} and χ_p (impurity of paramagnetism)= 0.2%, and for **6**, $g=2.1$, $2J=40.2$ (2) cm^{-1}, and $D=2.85(5)$ cm^{-1}. It is of interest to compare the structure and magnetism of the phenoxy-bridged complexes **4**–**7** series of $[FeL^2X]_2$, for which decreasing the strength of the antiferromagnetic interaction was found to coincide with increasing the Cu–O–Cu bond angle. The fitted $2J$ values for the complexes **4** ($X=NO_3^-$), **5** ($X=Cl^-$), and **7** ($X=NCS^-$) are -166, -480, and -320 cm^{-1}, respectively, and their corresponding mean Cu–O–Cu angles are 101.10, 103.30, and 102.32°, respectively. It has been found that there is a good correlation between the intradimer coupling constant and the mean Cu–O–Cu bridge angle within the Cu_2O_2 subunits. According to this relationship, complex **6** ($X=N_3^-$) has the positive $2J$ value of 40.2 cm^{-1} so its mean Cu–O–Cu angle would be expected to be smaller than that of complex **4**. Unfortunately no X-ray crystallographic data of **6** is available to examine this relationship.

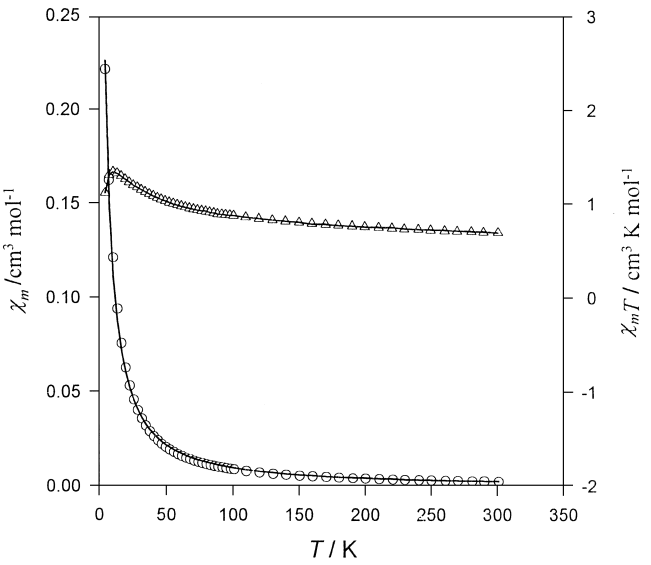

Fig. 4. Plots of χ_m (○) and $\chi_m T$ (△) versus T for complex **6**. The solid line is the fit provided by theoretical method (see text).

3.5. Electronic spectra and catalytic activity for the oxidation of H_2dtbc

The UV-Vis spectra of the 2×10^{-3} M solutions of the complexes **1**–**8** in methanol before addition of 3,5-dtbc were recorded in the range 200–800 nm. The electronic spectra for complexes **1**–**3** have been reported previously [25]. The representative spectra for complexes **4**–**7** of $[Cu(L^2)X]_2$ are shown in Fig. 5. The high-energy region of the spectra is characterized by the occurrence of an intense band around 360 nm, which may be assigned to the ligand ($L^2\pi$)-to-metal charge-transfer (LMCT) bands. As shown

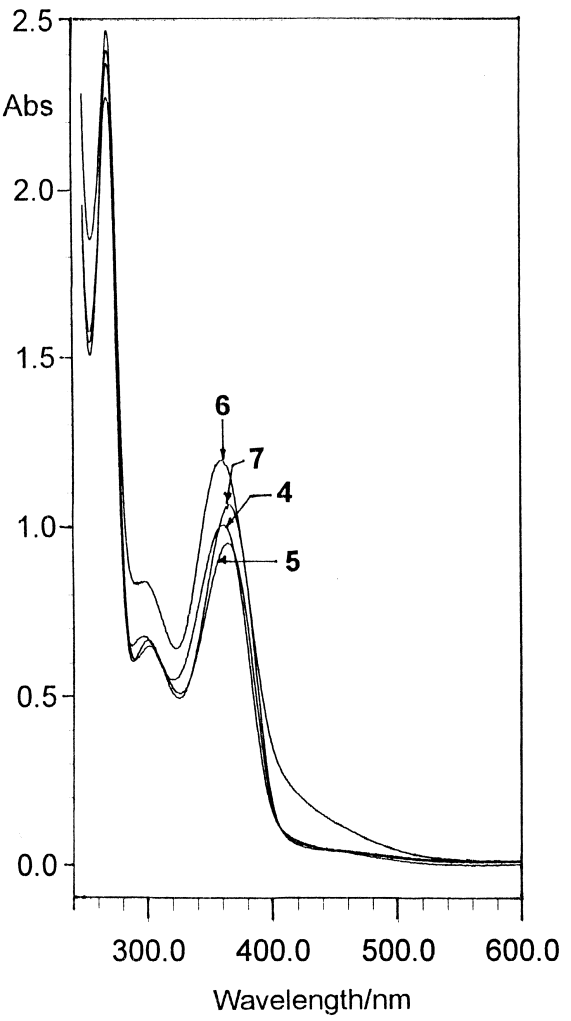

Fig. 5. The UV/Vis absorption spectra of 2×10^{-3} M solutions (in methanol) of complexes **4**–**7**.

in Fig. 6, 30 min after addition of 3,5-di-*tert*-butylcatechol (3,5-dtbc) (5 mM) to solutions (5×10^{-5} M) of the complex **4,** the main peak of the LMCT band at 360 nm vanishes. Simultaneously, the product 3,5-di-*tert*-butyl-*o*-quinone (3,5-dtbq) absorption at ~400 nm appears. Overall the time dependence of the quinone absorption under the studied conditions for complexes **1**–**3** and **4**–**7** series is linear as shown in Figs. 7 and 8, respectively. In addition, although the time dependence of the *o*-quinone absorption under the same conditions for complex **8** is linear, it shows little catecholase-like activity compared with the others in the present system. These results reveal a catecholase activity order of **3**≥**4**>**5**>**2**>**6**>**1**>**7**>**8**. This trend correlates to the Cu···Cu distances in complexes **1**–**8**, with the exception of **6**, as depicted in Fig. 9. The complexes **3** and **4,**with Cu–Cu distances of 2.928 and 3.008 Å, respectively, show the comparatively highest catecholase-like activity for all complexes in this study. Complex **8** has the lowest catecholase activity in all complexes. This may be due to either its large Cu···Cu

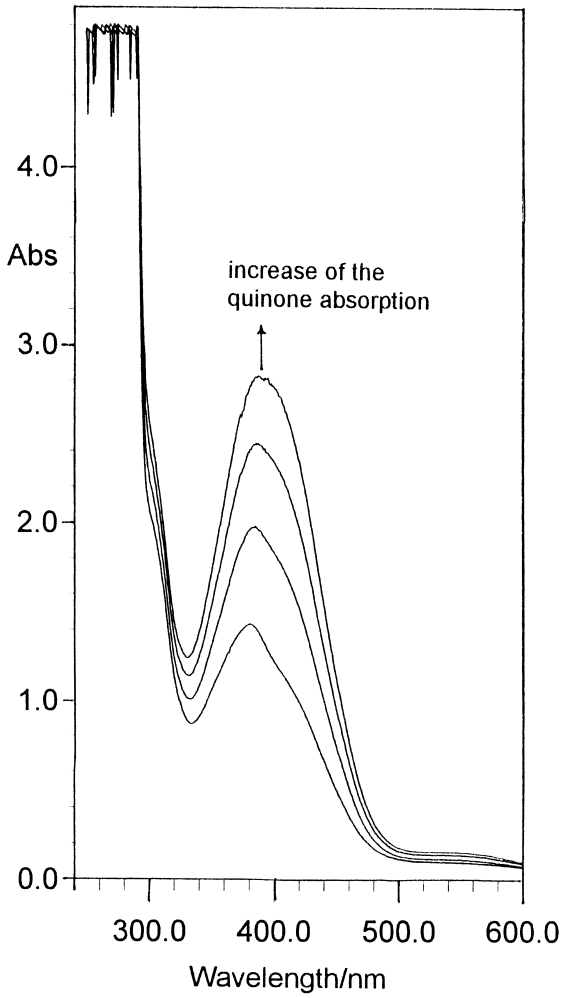

Fig. 6. Increase of the quinone band at 400 nm after addition of H_2dtbc (5 mM) to a solution of complex **4** (5×10^{-5} M) in methanol. The spectra were recorded every 30 min.

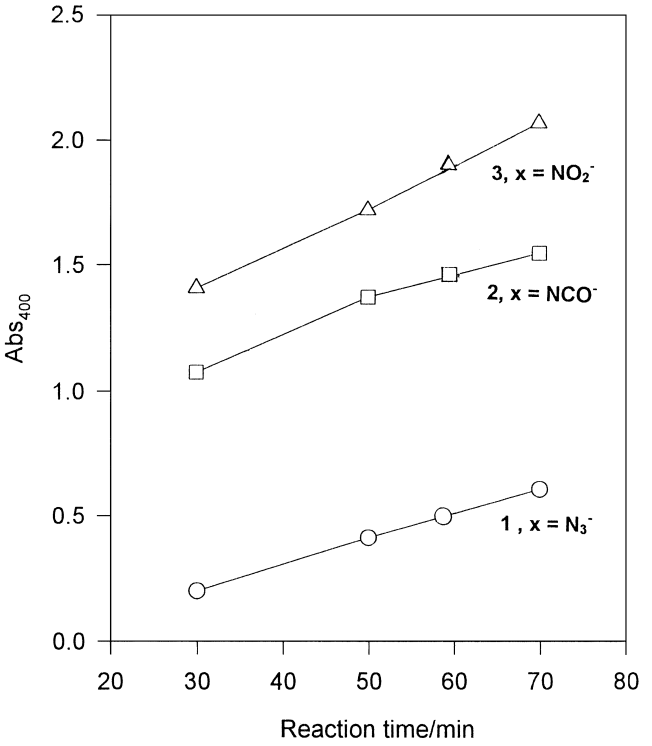

Fig. 7. The increase in quinone absorption at 400 nm with reaction time for the addition of H_2dtbc (5 mM) to 5×10^{-5} M solutions of complexes **1**–**3**.

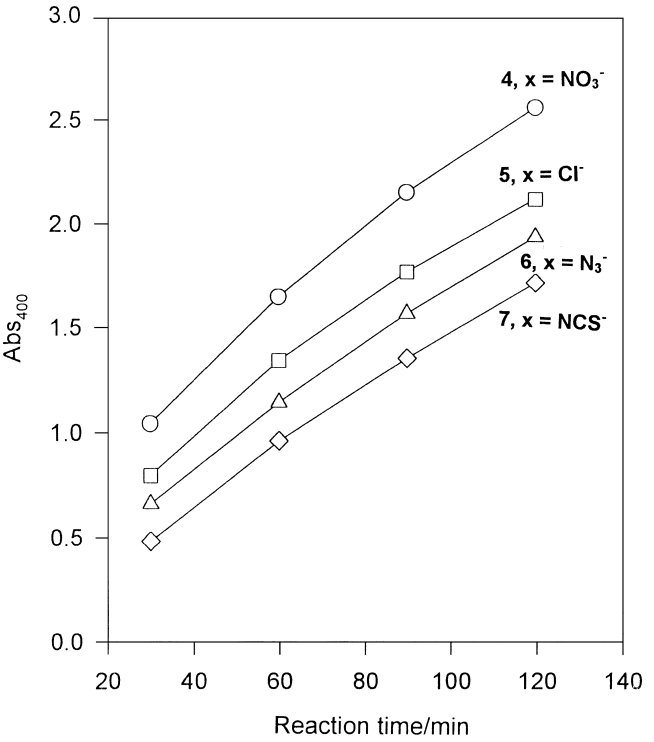

Fig. 8. The increase in quinone absorption at 400 nm with reaction time for the addition of H_2dtbc (5 mM) to 5×10^{-5} M solutions of complexes **4**–**7**.

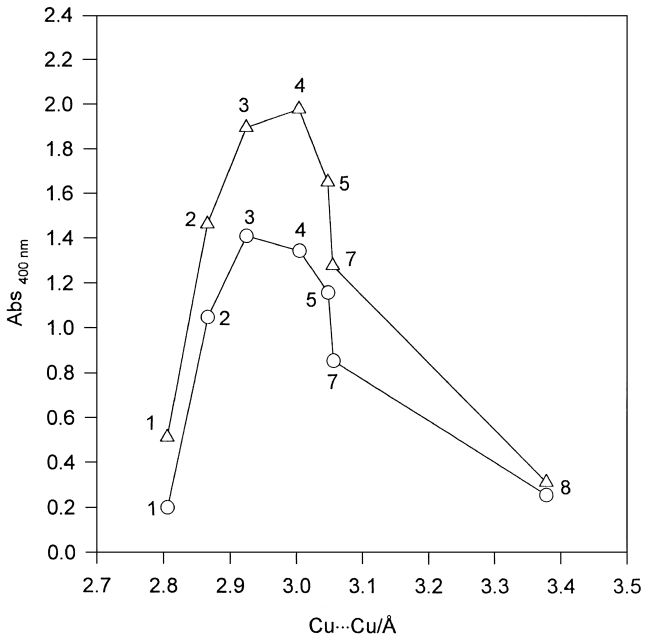

Fig. 9. Plot of Cu···Cu bond distances versus the values of absorbency of the quinone band at 400 nm (a) 30 min (– ○ –) and (b) 60 min (– △ –) after addition of H_2dtbc (5 mM) to 5×10^{-5} M solutions of complexes **1**–**5** and **7** and **8**.

distance or structural hindrance. A steric match between substrate and complex is believed to be important as determined by the features of two metal centres, which have to be located in proximity to facilitate binding of two hydroxyl oxygen atoms of catechol prior to the electron transfer [17–22]. The low catecholase activity of the complexes **1**, **6,** and **7** with $X=N_3^-$ and NCS^- in the present system implies some inhibitory activity of these ions in the reaction. This is consistent with the finding that the azide or thiocyanate ions are effective inhibitors in the function of the multi-copper binding sites of native metalloenzymes [1–10]. It is noteworthy that we have examined the ESR absorption spectra of complexes **1**–**8** in solid sate and in methanol solution (before addition of 3,5-dtbc), and revealed that the complexes, exception of complexes **1**, **6**, and **8**, are ESR silent due to strong antiferromagnetic exchange interactions between two Cu(II) ions in dinuclear complexes. Complexes **1**, **6**, and **8** exhibit a weak ESR absorption band at $g\sim2.0$, in which **1**, **6** exhibit weak ferromagnetic exchange interactions and **8** exhibit a vary weak antiferromagnetic exchange interaction between two Cu(II) ions in solid state, respectively. The results give an evidence that the complexes remain dimeric in methanol solution. Furthermore, after complete reaction of the complexes in methanol solution after addition of 3,5-dtbc, there also no ESR signal are observed, which may due to reduction of Cu(II) ions. However, the detailed mechanistic studies on the present system are currently in progress in our laboratory, which will give us to understand more details about the structure–function correlation of the catecholase-like reaction. In addition, the detailed mechanistic studies on the present system are currently in progress in our laboratory, which will give us to understand more details about the structure–function correlation of the catecholase-like reaction.

Acknowledgements

This research was supported by the National Science Council of Taiwan through Grant NSC-88-2113-M032-002. We are grateful for this financial support.

References

[1] K.D. Karlin, Z. Tyeklar (Eds.), Bioinorganic Chemistry of Copper, Chapman and Hall, New York, 1993.
[2] E.I. Solomon, M.J. Baldwin, M.D. Lowery, Chem. Rev. 92 (1992) 521–542.
[3] B. Reinhammer, in: Copper Proteins and Copper Enzymes, Vol. 3, CRC, Boca Raton, FL, 1984, pp. 1–35.
[4] T.G. Spiro, Copper Proteins, Wiley, New York, 1981.
[5] K.A. Magnus, H. Ton-That, J.E. Carpenter, Chem. Rev. 94 (1994) 727–735.
[6] E.I. Solomon, U.M. Sundaram, T.E. Mackonkin, Chem. Rev. 96 (1996) 2563–2605.
[7] N. Kitajima, Y. Moro-Oka, Chem. Rev. 94 (1994) 737–757.
[8] S. Ryan, H. Adams, D.E. Fenton, M. Becker, S. Schindler, Angew. Chem. Int. Ed. 37 (1998) 2134–2140.
[9] P.L. Holland, W.B. Tolman, Coord. Chem. Rev. 190–192 (1999) 855–869.
[10] H. Decker, R. Dillinger, F. Tuczek, Angew. Chem. Int. Ed. 39 (2000) 1591–1595.
[11] A. Rompel, H. Fischer, K. Büldt-Karentzopoulos, D. Meiwes, F. Zippel, H.F. Nolting, C. Hermes, B. Krebs, H. Witzel, J. Inorg. Biochem. 59 (1995) 715–718.
[12] B. Krebs, K. Büldt-Karentzopoulos, C. Eicken, A. Rompel, H. Witzel, A. Feldmann, R. Kruth, J. Reim, W. Steinforth, S. Teipel, F. Zippel, S. Schindler, F. Wiesemann, in: A.X. Trautwein (Ed.), Bioinorganic Chemistry: Transition Metals in Biology and Their Coordination Chemistry, VCH, Weinheim, 1997, pp. 616–631.
[13] C. Eicken, F. Zippel, K. Büldt-Karentzopoulos, B. Krebs, FEBS Lett. 436 (1998) 293–299.
[14] T. Klabunde, C. Eicken, J.C. Sacchettini, B. Krebs, Nat. Struct. Biol. 5 (1998) 1084–1090.
[15] P.L. Holland, W.B. Tolman, Coord. Chem. Rev. 190–192 (1999) 855–869.
[16] N. Oishi, Y. Nishida, K. Ida, S. Kida, Bull. Chem. Soc. Jpn. 53 (1980) 2847–2850.
[17] M.R. Malachowski, M.G. Davidson, Inorg. Chim. Acta 162 (1989) 199–204.
[18] K.D. Karlin, Y. Gultneh, T. Nicholson, J. Zubieta, Inorg. Chem. 24 (1985) 3725–3727.
[19] M.R. Malachowski, H.B. Huynh, L.J. Tomlinson, R.S. Kelly, J.W. Furbee Jr., J. Chem. Soc., Dalton Trans. (1995) 31–36.
[20] J. Manzur, A.M. Garcia, V. Rivas, A.M. Atria, J. Valenzuela, E. Spondine, Polyhedron 16 (1997) 2299–2305.
[21] F. Zippel, F. Ahlers, R. Werner, W. Haase, H.F. Nolting, B. Krebs, Inorg. Chem. 35 (1996) 3409–3419.
[22] J. Reim, B. Krebs, J. Chem. Soc., Dalton Trans. (1997) 3793–3804.
[23] E. Monzani, L. Quinti, A. Perotti, L. Casella, M. Gulloti, L.

Randaccio, S. Geremia, G. Nardin, P. Faleschini, G. Tabbi, Inorg. Chem. 37 (1998) 553–562.
[24] E. Monzanni, G. Battaini, A. Perotti, L. Casella, M. Gullotti, L. Santagostini, G. Nardin, L. Randaccio, S. Geremia, P. Zanello, G. Opromolla, Inorg. Chem. 38 (1999) 5359–5369.
[25] Y.H. Chung, H.H. Wei, Y.H. Liu, G.H. Lee, Yu Wang, J. Chem. Soc., Dalton. Trans. (1997) 2825–2829.
[26] E. Sinn, J. Chem. Soc., Chem. Commun. (1975) 665–666.
[27] E. Sinn, Inorg. Chem. 15 (1976) 358–365.
[28] O. Kahn, Molecular Magnetism, VCH, New York, 1993, P3.
[29] G.M. Sheldrick, SHELXL-93: Program for the Refinement of Crystal Structures, University of Gottingen, Germany, 1993.
[30] E. Sinn, Inorg. Chem. 15 (1976) 366–369.
[31] A.M. Countryman, W.T. Robinson, E. Sinn, Inorg. Chem. 13 (1974) 2013–2020.
[32] C.J. O'Connor, Prog. Inorg. Chem. 29 (1982) 203–283.
[33] O. Kahn, Molecular Magnetism, VCH, New York, 1993, P137-138.